RSC Advances

PAPER

View Article Online
View Journal | View Issue

Check for updates

Cite this: *RSC Adv.*, 2019, **9**, 31460

# Durable, acid-resistant copolymers from industrial by-product sulfur and microbially-produced tyrosine†

Timmy Thiounn,[a] Andrew G. Tennyson [ab] and Rhett C. Smith [*a]

The search for alternative feedstocks to replace petrochemical polymers has centered on plant-derived monomer feedstocks. Alternatives to agricultural feedstock production should also be pursued, especially considering the ecological damage caused by modern agricultural practices. Herein, L-tyrosine produced on an industrial scale by *E. coli* was derivatized with olefins to give tetraallyltyrosine. Tetraallyltyrosine was subsequently copolymerized *via* its inverse vulcanization with industrial by-product elemental sulfur in two different comonomer ratios to afford highly-crosslinked network copolymers $TTS_x$ ($x$ = wt% sulfur in monomer feed). $TTS_x$ copolymers were characterized by infrared spectroscopy, elemental analysis, thermogravimetric analysis, differential scanning calorimetry, and dynamic mechanical analysis (DMA). DMA was employed to assess the viscoelastic properties of $TTS_x$ through the temperature dependence of the storage modulus, loss modulus and energy damping ability. Stress–strain analysis revealed that the flexural strength of $TTS_x$ copolymers (>6.8 MPa) is more than 3 MPa higher than flexural strengths for previously-tested inverse vulcanized biopolymer derivatives, and more than twice the flexural strength of some Portland cement compositions (which range from 3–5 MPa). Despite the high tyrosine content (50–70 wt%) in $TTS_x$, the materials show no water-induced swelling or water uptake after being submerged for 24 h. More impressively, $TTS_x$ copolymers are highly resistant to oxidizing acid, with no deterioration of mechanical properties even after soaking in 0.5 M sulfuric acid for 24 h. The demonstration that these durable, chemically-resistant $TTS_x$ copolymers can be prepared from industrial by-product and microbially-produced monomers *via* a 100% atom-economical inverse vulcanization process portends their potential utility as sustainable surrogates for less ecofriendly materials.

Received 9th August 2019
Accepted 18th September 2019

DOI: 10.1039/c9ra06213k

rsc.li/rsc-advances

Open Access Article. Published on 03 October 2019. Downloaded on 12/29/2025 7:15:43 AM.
This article is licensed under a Creative Commons Attribution-NonCommercial 3.0 Unported Licence.

## Introduction

Polymers are ubiquitous in nearly every aspect of modern society to the extent that each person consumes 50 kg of polymers per year in Europe and 68 kg per year in the United States.[1] The vast majority of these polymers are made from petrochemicals and are relatively inert to typical biological degradation processes over any reasonable timeframe.[2] As a result, anthropogenic polymers accumulate in the environment in landfills, as floating masses and microplastic in the oceans,[3–5] and they have even begun to assimilate into landmasses through the formation of "plasticrust" around island shores.[6] Plant-derived monomers have been widely pursued as replacements for petrochemicals in the quest to find sustainable and degradable alternatives to polymers of the petrochemical century.[7,8] Agricultural production of crops for chemical feedstocks, however, comes with its own set of ecological problems, as modern agricultural practices wreak havoc on global phosphorus and nitrogen cycles and contaminate water resources through fertilizer and pesticide-laced runoff. Thus, whereas it is certainly imperative that agricultural waste products be leveraged for environmentally and economically advantageous uses, technological advances that rely on increased agricultural activities for the sole purpose of providing a new chemical feedstock should be weighed cautiously.

Some attractive alternatives to agricultural production of chemical feedstocks are to employ high production-density aquaculture of algae[9,10] or engineered bacteria[11–16] to produce target feedstocks. Such processes can be carried out in a closed system often operating at or slightly above ambient temperatures, thus limiting environmental impact and energy consumption.[17]

Regardless of how they are produced, chemically-resistant polymers often pose an environmental threat in terms of degradability, yet chemical resistance is required for many applications. New advances in production of chemically-

[a]*Department of Chemistry and Center for Optical Materials Science and Engineering Technologies, Clemson University, Clemson, South Carolina, USA. E-mail: rhett@clemson.edu*

[b]*Department of Materials Science and Engineering, Clemson University, Clemson, South Carolina, USA*

† Electronic supplementary information (ESI) available: Infrared spectra of $TTS_{30}$, $TTS_{50}$, and tetraallyltyrosine; DSC curves of $TTS_{30}$ and $TTS_{50}$. Trials 1–3 of stress strain measurements of $TTS_x$. See DOI: 10.1039/c9ra06213k



This journal is © The Royal Society of Chemistry 2019

Open Access Article. Published on 03 October 2019. Downloaded on 12/29/2025 7:15:43 AM.
This article is licensed under a Creative Commons Attribution-NonCommercial 3.0 Unported Licence.

resistant polymers should therefore centre on materials that are recyclable, and/or which degrade to environmentally benign compounds. High sulfur-content materials produced by inverse vulcanization of sustainable olefins have emerged recently as promising candidates in this regard.[18,19]

In the inverse vulcanization process,[20] sulfur, itself an industrial by-product of fossil fuel refining,[21–23] is simply heated with the requisite olefin to form crosslinked network solids with 100% atom economy (Scheme 1).[24–27] Many high sulfur-content materials can be remelted and recast over multiple cycles without loss of mechanical strength, and the environmental degradation products can be so environmentally benign that inverse vulcanization products have been used as fertilizers to improve the growth of food crops.[28,29] High sulfur-content composites can also exhibit remarkably high mechanical strength. Sulfur composites with lignin[30] or cellulose,[31] for example, have shown flexural strengths on par with that of Portland cement.

For the current work, tyrosine was an attractive initial feedstock because it is produced on an industrial scale by engineered strains of *E. coli*.[32–35] Furthermore, tyrosine is readily functionalized with four allyl groups, providing up to eight sites for the formation of C–S crosslinks upon inverse vulcanization (Scheme 2). The mechanical strength of high sulfur-content materials produced by inverse vulcanization increases with increased crosslink density,[30,31,36] so it was hypothesized that the high crosslink density provided by tetraallyltyrosine would likewise lead to durable copolymers. Inverse vulcanization of tetraallyltyrosine with sulfur was thus undertaken to produce crosslinked network copolymers **TTS$_x$** ($x$ = wt% sulfur in the monomer feed). Characterization by infrared spectroscopy, thermogravimetric analysis, differential scanning calorimetry, and dynamic mechanical analysis are discussed for **TTS$_x$** having two different monomer feed compositions. The resistance of **TTS$_x$** to water uptake and degradation by sulfuric acid are also assessed.

## Results and discussion

### Synthesis of TTS$_x$

A commercial sample of L-tyrosine produced by an engineered strain of *E. coli* was selected as the initial starting material for crosslinking with industrial by-product sulfur for the current study. Crosslinking of sulfur by inverse vulcanization requires an olefin-derivatized comonomer, so L-tyrosine was first converted to tetraallyltyrosine by the reported method (Scheme 2; NMR spectra provided in Fig. S1–S5 of the ESI†).[37] At STP, elemental sulfur exists primarily as $S_8$ rings in an orthorhombic crystal morphology. Upon heating, $S_8$ first melts at 118 °C and then forms polymeric sulfur radicals at temperatures > 159 °C

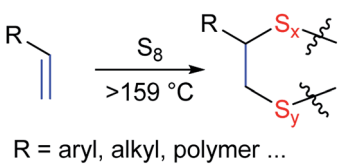


Scheme 1 General inverse vulcanization strategy.

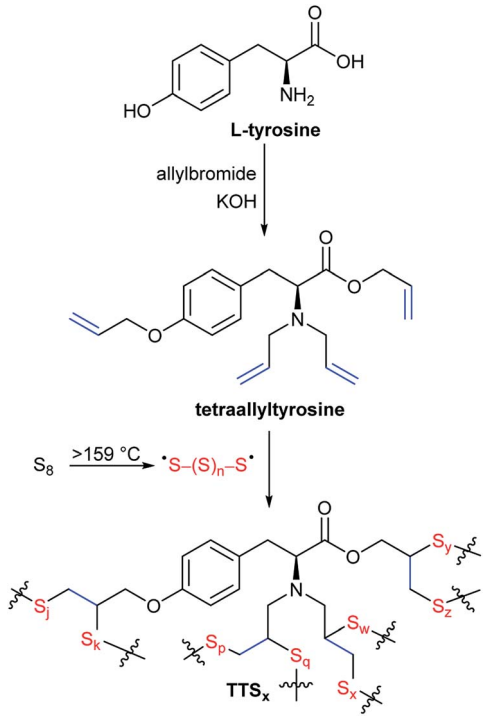


Scheme 2 Preparation of tetraallyltyrosine and its inverse vulcanization to yield TTS$_x$.

(Scheme 2).[38] These polymeric sulfur radicals are thought to be the active species for reaction with olefins to form crosslinks. In the current case, reaction between sulfur radicals and the four olefin moieties of tetraallyltyrosine affords up to eight S–C crosslinks per molecule. Upon heating a sample of tetraallyltyrosine and sulfur above 159 °C, the solution initially was the dark red colour characteristic of polymeric sulfur radicals and then transformed to a deep brown-red liquid within 5 min. When the sulfur: tetraallyltyrosine mass ratio was >1, the reaction mixture did not homogenize even after extended stirring and heating. Instead, a dark-coloured solid ball of material precipitated from the liquid phase. The separated solid was comprised of sulfur-crosslinked tetraallyltyrosine, whereas the cooled liquid phase was unreacted $S_8$. For reactions in which the sulfur: tetraallyltyrosine mass ratio was ≤1, dark red-brown, homogeneous reaction solutions were observed after 30–45 minutes of heating. Two sulfur: tetraallyltyrosine monomer mixtures, comprised of 50 wt% and 30 wt% sulfur, were thus selected for further investigation to produce **TTS$_{50}$** and **TTS$_{30}$**, respectively.

In contrast to many reported high sulfur-content materials,[30,31,36,39,40] once **TTS$_{50}$** or **TTS$_{30}$** were set as solids they could not be remelted or reshaped. To prepare materials of desired shapes, it was necessary to pour the homogenized reaction solutions into a mould for subsequent heating to complete the crosslinking process. Moulded samples of **TTS$_x$** prepared in this manner were hard, dark red-brown, semi-transparent solids with smooth, shiny surfaces (Fig. 1). The densities of the materials so produced (1.2–1.3 g cm$^{-3}$) are somewhat higher than that of a typical organic polymer by merit of the high sulfur content, given that the density of pure sulfur is 2 g cm$^{-3}$. Infrared spectra

Open Access Article. Published on 03 October 2019. Downloaded on 12/29/2025 7:15:43 AM.
This article is licensed under a Creative Commons Attribution-NonCommercial 3.0 Unported Licence.

Fig. 1 Shaped materials can be fabricated from $TTS_x$ thermosets by curing the comonomer solution at 150 °C in a mould or on a substrate, as illustrated by the rectangular prismatic brick (left) and patterned disc-shaped item (centre). A backlit sample of $TTS_x$ (right) better illustrates the red colour and transparency of the material.

(Fig. S6, ESI†) of $\mathbf{TTS_x}$ reveals near complete loss of the mono-substituted alkene C–H bending mode (920 and 995 $cm^{-1}$) from the allyl group in tetraallyltyrosine upon reaction with sulfur, demonstrating the efficiency of the crosslinking process.

Some high sulfur-content materials prepared by inverse vulcanization are homogeneous copolymer networks, while others are composites wherein free sulfur occupies voids in a sulfur-crosslinked network polymer.[28,30,31] Free sulfur is quite soluble in $CS_2$, whereas the crosslinked network is insoluble, so recursive rinsing of $\mathbf{TTS_x}$ with $CS_2$ was undertaken to extract any free sulfur. A minimal amount of the material was extractable from $\mathbf{TTS_x}$ by this method (15 and 11% for $\mathbf{TTS_{30}}$ and $\mathbf{TTS_{50}}$, respectively), and the elemental analysis of the soluble fraction matched that of the bulk material, rather than being free sulfur. Differential scanning calorimetry (DSC, *vide infra*) data likewise did not show thermal transitions associated with free sulfur. These data support the characterization of $\mathbf{TTS_x}$ as consisting primarily of sulfur-crosslinked networks without appreciable free sulfur present, as they are depicted in Scheme 2. Considering near complete consumption of alkene units and the limited amount of free sulfur in each material, the average crosslink was calculated to consist of about 6 or 3 sulfur atoms in $\mathbf{TTS_{30}}$ and $\mathbf{TTS_{50}}$, respectively. The short average crosslink length provides an explanation for the observation that $\mathbf{TTS_x}$ cannot be remelted. The ability to re-melt high sulfur-content materials generally relies on the thermal reversibility of S–S bond formation. With an average crosslink length of only 3–6 sulfur atoms, a significant fraction of crosslinks will comprise a single sulfur atom, and thus lack the S–S bond needed for reversible bond-formation. The high crosslink density in these materials thus unfortunately precludes $\mathbf{TTS_x}$ from the re-melting exhibited by materials having longer average oligo-sulfur crosslink lengths.

### Thermal properties of $TTS_x$

The thermogravimetric analysis (TGA) data (Table 1 and Fig. 2) reveal that the onset of decomposition for the starting materials, tetraallyltyrosine and sulfur are 182 and 282 °C respectively, and both have char yields of <1%. The decomposition temperatures ($T_d$) for $\mathbf{TTS_{30}}$ (209 °C) and $\mathbf{TTS_{50}}$ (211 °C) lie between those for tetraallyltyrosine and sulfur. The char yields for $\mathbf{TTS_x}$ materials also show a significant increase from the initial monomers, with an increase to 23–26%.

Table 1 Summary of properties of materials

| | $\mathbf{TTS_{30}}$ | $\mathbf{TTS_{50}}$ |
|---|---|---|
| $T_d$ (°C)[a] | 209 | 211 |
| Char yield | 26% | 23% |
| $T_g$[b] (°C) | 68 | 58 |
| $E' T_g$[c] (°C) | 48.4 | 47.0 |
| $E'' T_g$[d] (°C) | 60.8 | 58.2 |
| tan $\delta$ $T_g$[e] (°C) | 77.2 | 70.5 |
| Density (g $cm^{-3}$) | 1.3 ± 0.1 | 1.2 ± 0.1 |
| $H_2O$ uptake | <0.5%[f] | <0.5%[f] |

[a] Determined from the onset of the major mass loss peak. [b] Determined from the onset of transition from the second heating cycle of the DSC curve. [c] Determined from the onset of the storage modulus. [d] Determined from the peak of the loss modulus curve. [e] Determined from the peak of tan $\delta$ curve. [f] No measurable water uptake.

Differential scanning calorimetry was also used to assess the thermal and morphological properties of $\mathbf{TTS_x}$ (Fig. S7†). The glass transition temperatures ($T_g$) of $\mathbf{TTS_{30}}$ (68 °C) and $\mathbf{TTS_{50}}$ (58 °C) are both well above room temperature, while the higher $T_g$ of $\mathbf{TTS_{30}}$ reflects fewer degrees of freedom in the more-crosslinked material. Notably, the DSC traces for $\mathbf{TTS_x}$ do not exhibit a melt peak for orthorhombic sulfur, in agreement with the observation of very little $CS_2$-extractable free sulfur. In contrast, the DSC traces for high sulfur-content composites from which significant quantities of free sulfur are extractable exhibit prominent peaks at 116–120 °C attributable to orthorhombic sulfur melting transitions.[30,31,36] Peaks attributable to polymeric sulfur domains are also notably absent from the DSC traces of $\mathbf{TTS_x}$. Polymeric sulfur domains generally produce endothermic transitions at around −37 °C and sometimes also cold crystallization peaks over a broad temperature range of −20 to +40 °C.[30,31] the absence of such features in the DSC analysis of $\mathbf{TTS_x}$ further confirms the short average crosslink length.

### Mechanical properties and chemical resistance of $TTS_x$

The high crosslink density in $\mathbf{TTS_x}$ was hypothesized to endow them with high strength and durability. To test this hypothesis, $\mathbf{TTS_{30}}$ and $\mathbf{TTS_{50}}$ were subjected to dynamic mechanical analysis

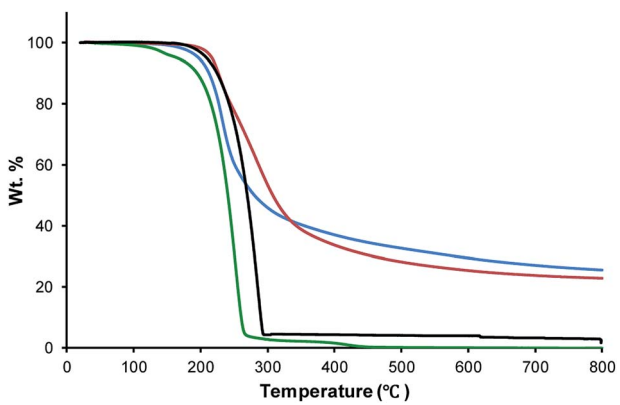


Fig. 2 Thermogravimetric analysis (TGA) traces for elemental sulfur (black trace), tetraallyltyrosine (green trace), $TTS_{30}$ (blue trace) and $TTS_{50}$ (red trace).


This journal is © The Royal Society of Chemistry 2019

Open Access Article. Published on 03 October 2019. Downloaded on 12/29/2025 7:15:43 AM.
This article is licensed under a Creative Commons Attribution-NonCommercial 3.0 Unported Licence.

(DMA). The temperature-dependences of storage modulus ($E'$), loss modulus ($E''$) and energy damping factor (tan $\delta$) were initially assessed (Fig. 3 and Table 1). Expectedly, the $E'$ is higher for **TTS$_{30}$** whereas the tan $\delta$ is higher for the less-densely-crosslinked **TTS$_{50}$**. The storage and loss moduli for both copolymers are significantly higher than those of uncrosslinked elemental sulfur, which is too brittle to even be clamped in the DMA instrument at the minimum clamping force.

Stress–strain analysis of **TTS$_{30}$** and **TTS$_{50}$** provides the flexural modulus and minimum flexural strength of **TTS$_x$** copolymers at room temperature (Fig. 4A and Table 2). The flexural storage modulus of **TTS$_{30}$** is greater than that of **TTS$_{50}$** (860 *vs.* 580 MPa), indicative of the higher crosslink density of the **TTS$_{30}$** sample. Additionally, the flexural strength for **TTS$_{30}$** is slightly greater than **TTS$_{50}$** sample. Note that because the samples did not break at the maximum force applicable by the instrument (10 N), these already high flexural strengths represent a minimum flexural strength for the materials. The flexural strengths of **TTS$_x$** exceed those of other sulfur-crosslinked materials for which stress–strain data have been reported, including cellulose/sulfur (up to 3.8 MPa) and lignin/sulfur composites (up to 2.1 MPa). For comparison to a more familiar material, the flexural strength of Portland cement ranges from 3–5 MPa. Other materials utilizing sulfur with dicyclopentadiene, linseed oil, and canola oil led to materials with flexural strengths of up to 6 MPa.[41] The **TTS$_x$** materials exhibit flexural strengths in excess of 7.0 MPa; this is a lower limit because samples do not break at maximum instrument force. The high strength may be attributable to higher crosslink density afforded by tetraallyltyrosine, which features eight potential sites for crosslinking per molecule.

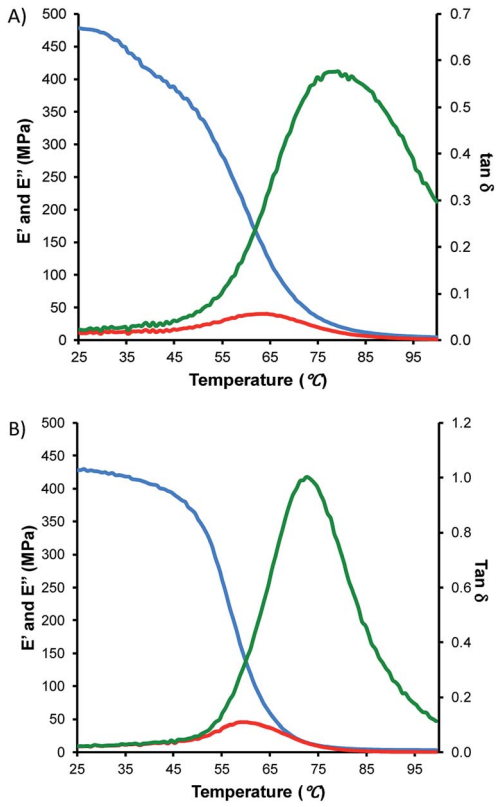


Fig. 3 Storage modulus ($E'$, blue trace), loss modulus ($E''$, red trace) and damping factor (tan $\delta$, green trace) for TTS$_{30}$ (A) and TTS$_{50}$ (B).

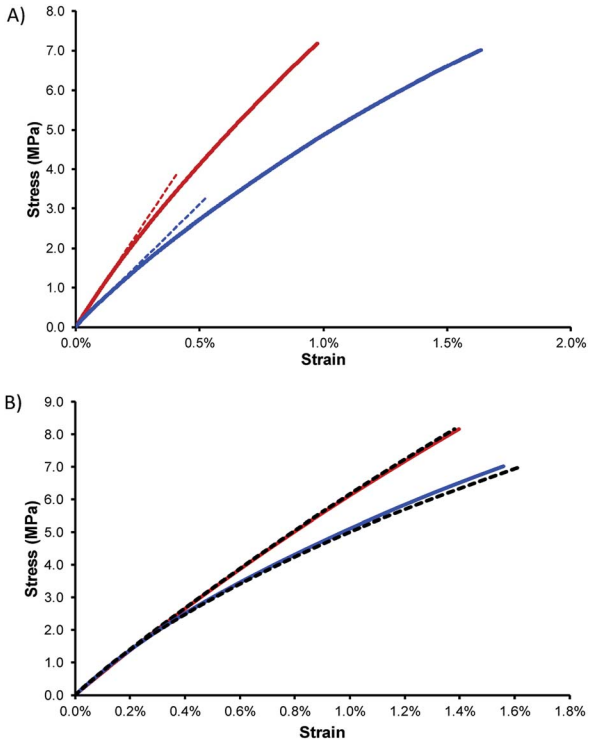


Fig. 4 (A) Stress–strain analysis for TTS$_{30}$ (red trace) and TTS$_{50}$ (blue trace). The dashed lines are propagations of the linear regions of the respective stress strain curves. (B) Comparison of stress–strain analysis for TTS$_{30}$ (red trace) and TTS$_{50}$ (blue trace) before (solid traces) and after (coincident black dashed traces) exposure to sulfuric acid for 24 h.

With such a high content of tyrosine-derived monomer, water uptake and attendant swelling or loss of mechanical integrity could be a concern for **TTS$_x$** materials. On the other hand, elemental sulfur is highly hydrophobic, with a critical surface energy of 27 mN m$^{-1}$, which is between the values for Teflon (24 mN m$^{-1}$) and polyethylene (32.6 mN m$^{-1}$).[42] Samples of **TTS$_x$** were thus weighed, submerged in water for 24 h, and reweighed after this soaking period. No water uptake or change in dimensions was measurable for either **TTS$_x$** sample,

Table 2 Summary of flexural properties of TTS$_x$ materials[a]

| Material | Flexural storage modulus (MPa) | Flexural strength (MPa) |
|---|---|---|
| **TTS$_{30}$** | 860 ± 110 | >7.0 ± 1 |
| After $H_2SO_4$[b] | 100% | 100% |
| **TTS$_{50}$** | 580 ± 140 | >6.8 ± 0.4 |
| After $H_2SO_4$[b] | 100% | 100% |

[a] Values determined from the average of three runs. [b] Percentage of initial metric retained after soaking the sample in 0.5 M $H_2SO_4$ (aq.) for 24 h.

Open Access Article. Published on 03 October 2019. Downloaded on 12/29/2025 7:15:43 AM. This article is licensed under a Creative Commons Attribution-NonCommercial 3.0 Unported Licence.

confirming exclusion of water by the hydrophobic sulfur. Water exclusion in polymers comprising polar functional groups is an important property given that uptake of even small quantities of water can significantly impact the mechanical properties of a material. The $T_g$ of nylon-6,6, for example, falls from 100 °C when dry to 43 °C after 3.5 wt% water uptake – occurring at a relative humidity of just 55% – and the tensile strength at yield falls concomitantly from 80 MPa to 43 MPa.[43] The mechanical strength of **TTS$_x$**, however, is unchanged even after being submerged in water for 24 h.

Whereas the ready decomposition of high sulfur-content materials by soil bacteria can be an asset from a sustainability standpoint, polymers having some targeted chemical resistance may be advantageous or required for a given application. Sulfur-infused masonry and cementitious materials, for example, have proven especially effective in applications requiring resistance to corrosion by acid.[44,45] To assess the extent to which **TTS$_x$** copolymers could maintain their structural integrity after challenge by acid exposure, a brick of each copolymer was soaked in 0.5 M $H_2SO_4$ (aq.) for 24 h and then the stress–strain curve was re-measured. Sulfuric acid was selected because it is a strong and oxidizing acid that reacts with many common organic functional groups. Impressively, neither **TTS$_{30}$** nor **TTS$_{50}$** showed any change in dimensions or flexural strength/modulus after challenge by sulfuric acid (Fig. 4B). This is an especially important finding because it demonstrates that at least 50 wt% tyrosine can be protected by sulfur crosslinking, whereas chemical susceptibility is a common criticism of bio-derived polymers comprising polar functional groups as compared to many common petrochemical polymers.

# Conclusions

Durable, chemically-resistant **TTS$_x$** copolymers have been prepared from industrial by-product sulfur and a derivative of microbially-produced L-tyrosine *via* the 100% atom-economical inverse vulcanization process. The copolymers are highly-crosslinked network copolymers comprised primarily of sulfur-crosslinked tetraallyltyrosine wherein the average crosslinks are 3–6 sulfur atoms in length. The flexural strengths of **TTS$_x$** copolymers are significantly higher than that of Portland cement. Despite the high tyrosine content (50–70 wt%), the copolymers exhibit no swelling, water uptake or deterioration of mechanical properties even after soaking in 0.5 M aqueous sulfuric acid for 24 h.

# Experimental

## General considerations

All NMR spectra were recorded on a Bruker Avance spectrometer operating at 300 MHz for proton nuclei. Fourier transform infrared spectra were obtained using a Shimadzu IR Affinity-1S instrument operating over the range of 400–4000 cm$^{-1}$ at ambient temperature. Thermogravimetric analysis (TGA) was recorded on a Mettler Toledo TGA 2 STAR$^e$ System over the range of 25 to 800 °C with a heating rate of 5 °C min$^{-1}$ under a flow of $N_2$ (20 mL min$^{-1}$). Differential Scanning Calorimetry (DSC) was acquired using a Mettler Toledo DSC 3 STAR$^e$ System over the range of 0 to 140 °C, with a heating rate of 5 °C min$^{-1}$ under a flow of $N_2$ (200 mL min$^{-1}$). Each DSC measurement was carried out over 3 heat-cool cycles to get rid of any thermal history. The data reported were taken from the second cycle of the experiment. Dynamic Mechanical Analysis (DMA) was performed using a Mettler Toledo DMA 1 STAR$^e$ System in single cantilever mode. DMA samples were cast from two stainless steel moulds with sample dimensions of approximately 2 × 11 × 40 mm and 2 × 11 × 19 mm. Temperature scans were taken with the smaller DMA sample while stress strain measurements were taken with the larger samples. The clamping force for both temperature scan and stress strain measurements was set to 1 cN m. Temperature scans were measured from 25–100 °C and the motor displacement was set to 5 μm and a free length of 5 mm. Static stress–strain measurements were taken at 25 °C in single cantilever mode with a force range of 0–10 N, a ramp rate of 0.1 N min$^{-1}$, and with a free length of 10 mm.

## Materials and methods

L-Tyrosine (99%, Alfa Aesar), allyl bromide (Oakwood Chemical), elemental sulfur (99.5%, Alfa Aesar) and potassium hydroxide (Fluka Analytical) were used without further purification. Tetraallyltyrosine was prepared as previously reported.[37]

Water uptake measurements were taken after soaking a sample of **TTS$_x$** in deionized water for 24 h. A sample of **TTS$_x$** was taken after the initial stress strain measurement, was re-run, followed by soaking in 0.5 M $H_2SO_4$ (aq.) solution for 24 h. After 24 h the sample was dried and subjected stress strain measurements.

## General synthesis of TTS$_x$

**CAUTION:** *Heating elemental sulfur with organics can result in the formation of $H_2S$ gas. $H_2S$ is toxic, foul-smelling, and corrosive.* Elemental sulfur and tetraallyltyrosine was weighed directly into a 20 mL scintillation vial. The vessel was placed in a thermostat-controlled oil bath set to 150 °C (the internal temperature rises to between 160 and 180 °C). After the sulfur began to melt, two visible layers were formed. The reaction media was vigorously stirred with a Teflon coated stir bar until the reaction mixture became homogenous (30–45 min). Once the reaction mixture became homogenous, the reaction solution was transferred to stainless steel moulds in a 150 °C oven to cure for 4 h. Reagent masses and results of elemental combustion microanalysis are provided below.

## Synthesis of TTS$_{30}$

The general synthesis above was used to synthesize **TTS$_{30}$** (30 wt% sulfur) where 3.01 g of elemental sulfur and 7.00 g of tetraallyltyrosine were used in the reaction, with a recovered yield of 95%. Elemental analysis calculated: C, 51.7%; S, 30.0%; H, 5.6%; N, 2.9%. Found: C, 49.6%; S, 33.4%; H, 5.4%; N, 2.9%.

## Synthesis of TTS$_{50}$

The general synthesis above was used to synthesize **TTS$_{50}$** (50 wt% sulfur) where 5.02 g of elemental sulfur and 5.02 g of

 This journal is © The Royal Society of Chemistry 2019

Open Access Article. Published on 03 October 2019. Downloaded on 12/29/2025 7:15:43 AM. This article is licensed under a Creative Commons Attribution-NonCommercial 3.0 Unported Licence.

tetraallyltyrosine were used in the reaction, with a recovered yield of 95%. Elemental analysis calculated: C, 36.9%; S, 50.0%; H, 4.0%; N, 2.1%. Found: C, 38.44%; S, 51.39%; H, 3.59%; N, 2.28%.

## Conflicts of interest

There are no conflicts to declare.

## Acknowledgements

This work was supported by the National Science Foundation (CHE-1708844).

## Notes and references

1 https://www.plasticsinsight.com/world-per-capita-consumption-pe-pp-pvc-resins-2014/, accessed 7-4-19.
2 R. Geyer, J. R. Jambeck and K. L. Law, *Sci. Adv.*, 2017, **3**, e1700782.
3 J. Jeong and J. Choi, *Chemosphere*, 2019, **231**, 249–255.
4 M. Cole, P. Lindeque, C. Halsband and T. S. Galloway, *Mar. Pollut. Bull.*, 2011, **62**, 2588–2597.
5 V. Hidalgo-Ruz, L. Gutow, R. C. Thompson and M. Thiel, *Environ. Sci. Technol.*, 2012, **46**, 3060–3075.
6 I. Gestoso, E. Cacabelos, P. Ramalhosa and J. Canning-Clode, *Sci. Total Environ.*, 2019, **687**, 413–415.
7 L. Lanni, *Infinity Line*, LMNO Press, Chapin, SC, USA, 2018.
8 S. L. Kristufek, K. T. Wacker, Y.-Y. Timothy Tsao, L. Su and K. L. Wooley, *Nat. Prod. Rep.*, 2017, **34**, 433–459.
9 N. Wei, J. Quarterman and Y.-S. Jin, *Trends Biotechnol.*, 2013, **31**, 70–77.
10 R. V. Durvasula, D. V. S. Rao and V. S. Rao, *Biotechnological Applications of Microalgae*, 2013, pp. 201–227.
11 Y. Zhang, A. Kumar, P. R. Hardwidge, T. Tanaka, A. Kondo and P. V. Vadlani, *Biotechnol. Prog.*, 2016, **32**, 271–278.
12 P. Nawabi, S. Bauer, N. Kyrpides and A. Lykidis, *Appl. Environ. Microbiol.*, 2011, **77**, 8052–8061.
13 S. Magdouli, S. Yan, R. D. Tyagi and R. Y. Surampalli, *Crit. Rev. Environ. Sci. Technol.*, 2014, **44**, 416–453.
14 C. E. d. F. Silva and A. Bertucco, *Process Biochem.*, 2016, **51**, 1833–1842.
15 M.-H. Liang and J.-G. Jiang, *Prog. Lipid Res.*, 2013, **52**, 395–408.
16 P. Majidian, M. Tabatabaei, M. Zeinolabedini, M. P. Naghshbandi and Y. Chisti, *Renewable Sustainable Energy Rev.*, 2018, **82**, 3863–3885.
17 B. Erickson, J. E. Nelson and P. Winters, *Biotechnol. J.*, 2012, **7**, 176–185.
18 D. J. Parker, S. T. Chong and T. Hasell, *RSC Adv.*, 2018, **8**, 27892–27899.
19 M. J. H. Worthington, R. L. Kucera and J. M. Chalker, *Green Chem.*, 2017, **19**, 2748–2761.
20 W. J. Chung, J. J. Griebel, E. T. Kim, H. Yoon, A. G. Simmonds, H. J. Ji, P. T. Dirlam, R. S. Glass, J. J. Wie, N. A. Nguyen, B. W. Guralnick, J. Park, A. Somogyi, P. Theato, M. E. Mackay, Y.-E. Sung, K. Char and J. Pyun, *Nat. Chem.*, 2013, **5**, 518–524.
21 X. Zhang, Y. Tang, S. Qu, J. Da and Z. Hao, *ACS Catal.*, 2015, **5**, 1053–1067.
22 A. Demirbas, H. Alidrisi and M. A. Balubaid, *Pet. Sci. Technol.*, 2015, **33**, 93–101.
23 G. Kutney, *Sulfur. History, Technology, Applications & Industry*, ChemTec, Toronto, 2007.
24 Y. Zhang, R. S. Glass, K. Char and J. Pyun, *Polym. Chem.*, 2019, **10**, 4078–4105.
25 J. M. Chalker, M. J. H. Worthington, N. A. Lundquist and L. J. Esdaile, *Top. Curr. Chem.*, 2019, **377**, 1–27.
26 M. K. Salman, B. Karabay, L. C. Karabay and A. Cihaner, *J. Appl. Polym. Sci.*, 2016, **133**, 43655.
27 J. J. Griebel, R. S. Glass, K. Char and J. Pyun, *Prog. Polym. Sci.*, 2016, **58**, 90–125.
28 M. Mann, J. E. Kruger, F. Andari, J. McErlean, J. R. Gascooke, J. A. Smith, M. J. H. Worthington, C. C. C. McKinley, J. A. Campbell, D. A. Lewis, T. Hasell, M. V. Perkins and J. M. Chalker, *Org. Biomol. Chem.*, 2019, **17**, 1929–1936.
29 S. F. Valle, A. S. Giroto, R. Klaic, G. G. F. Guimaraes and C. Ribeiro, *Polym. Degrad. Stab.*, 2019, **162**, 102–105.
30 M. Karunarathna, M. K. Lauer, T. Thiounn, R. C. Smith and A. G. Tennyson, *J. Mater. Chem. A*, 2019, **7**, 15683–15690.
31 M. K. Lauer, T. A. Estrada-Mendoza, C. D. McMillen, G. Chumanov, A. G. Tennyson and R. C. Smith, *Adv. Sustainable Syst.*, 2019, **3**, 1900062.
32 M. Ikeda, *Appl. Microbiol. Biotechnol.*, 2006, **69**, 615–626.
33 D. Na, S. M. Yoo, H. Chung, H. Park, J. H. Park and S. Y. Lee, *Nat. Biotechnol.*, 2013, **31**, 170–174.
34 T. Luetke-Eversloh, C. N. S. Santos and G. Stephanopoulos, *Appl. Microbiol. Biotechnol.*, 2007, **77**, 751–762.
35 M. I. Chavez-Bejar, J. L. Baez-Viveros, A. Martinez, F. Bolivar and G. Gosset, *Process Biochem.*, 2012, **47**, 1017–1026.
36 T. Thiounn, M. K. Lauer, M. S. Bedford, R. C. Smith and A. G. Tennyson, *RSC Adv.*, 2018, **8**, 39074–39082.
37 S. Aoyagi, T. Shimasaki, N. Teramoto and M. Shibata, *Eur. Polym. J.*, 2018, **101**, 151–158.
38 B. Meyer, *Chem. Rev.*, 1976, **76**, 367–388.
39 J. J. Griebel, N. A. Nguyen, S. Namnabat, L. E. Anderson, R. S. Glass, R. A. Norwood, M. E. MacKay, K. Char and J. Pyun, *ACS Macro Lett.*, 2015, **4**, 862–866.
40 A. D. Smith, T. Thiounn, E. W. Lyles, E. K. Kibler, R. C. Smith and A. G. Tennyson, *J. Polym. Sci., Part A: Polym. Chem.*, 2019, **57**, 1704–1710.
41 J. A. Smith, S. J. Green, S. Petcher, D. J. Parker, B. Zhang, M. J. H. Worthington, X. Wu, C. A. Kelly, T. Baker, C. T. Gibson, J. A. Campbell, D. A. Lewis, M. J. Jenkins, H. Willcock, J. M. Chalker and T. Hasell, *Chem.–Eur. J.*, 2019, **25**, 10433–10440.
42 S. Kelebek, *J. Colloid Interface Sci.*, 1988, **124**, 504–514.
43 C. C. Pai, R. J. Jeng, S. J. Grossman and J. C. Huang, *Adv. Polym. Technol.*, 1989, **9**, 157–163.
44 H. H. Weber Jr, *ACI Symposium Publication*, 1993, SP-137, pp. 49–72.
45 H. H. Weber and W. C. McBee, *New market opportunities for sulphur asphalt*, Washington, D.C., 2000.